

VASCULAR SYSTEM WITHIN DEVELOPING ROOT NODULES OF *LUPINUS LUTEUS* L. PART 1. JUVENILE STAGE**

BARBARA ŁOTOCKA*

Department of Botany, Warsaw University of Life Sciences,
Nowoursynowska 159, 02-776 Warsaw, Poland

Received December 27, 2007; revision accepted February 15, 2008

The ontogeny and (ultra)structure of vascular tissue in *Lupinus luteus* L. root nodules were studied by light and transmission electron microscopy in juvenile nodule primordia up to the 11th day after inoculation. Vascular meristem originated from centripetally dedifferentiated root cortical parenchyma, endodermis and pericycle. The vascular trace was formed between bacteroid tissue initials and the root stele. In the trace's proximal part, cambial strands connecting the vascular trace and root cambium were formed. In the distal part, non-anastomosing vascular bundles started differentiating from the trace at the end of the juvenile stage. In lupine, the formative stage of the indeterminate root nodule vascular system was shown to be unique within the legumes.

Key words: Endodermis, *Lupinus luteus* L., phloem, root nodule, root nodule development, transfer cells, vascular meristem, vascular tissue, xylem.

INTRODUCTION

Legume/rhizobia symbiosis results in the formation of root nodules. Nodulation is widely investigated in various aspects, including signal transduction, cell cycle control, gene expression and tissue differentiation (Hirsch, 1992). The root nodule is a construct of three principal tissues: protective, bacteroid and vascular. The last one is the least studied and least understood. The presence of vascular strands in root nodules was recognized already by 18th-century anatomists (Fred et al., 1932), but closer examination was largely neglected later. Pate et al. (1969) made a broad survey of nodule vascular tissue structure and function, and Briarty (1978) analyzed the development of xylem transfer cells in clover root nodules. The gap in the data on the root nodule vascular system is somewhat surprising in view of the crucial role of vascular tissue in nodule physiology. Via the nodule vascular system, nutrients yielding energy and carbon skeletons for nitrogen fixation are imported to the nodule, while the products of N₂ fixation are exported. Proper performance of both functions is fundamental to the rhizobium/host-plant relationship (Brenchley and Thornton, 1925; Fraser, 1942).

In *Lupinus luteus* L. the nodules contain a persistent meristem; that is, they are of indeterminate type. In regard to their developmental anatomy,

which is unique among legume plants, a general outline of nodule formation was described, as well as the initial stages of nodule primordium formation, differentiation of bacteroid tissue, and the effects of mutation in the microsymbiont's *nolL* or *nodZ* genes upon nodule structure (Golinowski et al., 1987; Łotocka et al., 1995; Łotocka et al., 2000a; Golinowski et al., 1992; Łotocka et al., 2000b, respectively). The present work examines vascular system formation, which is especially extensive and complex in the root nodules of *L. luteus*; this paper reports observations of early stages.

MATERIALS AND METHODS

GROWTH CONDITIONS

Seeds of *Lupinus luteus* L. cv. Ventus were germinated aseptically, and seedling roots ~2 cm long were inoculated with *Bradyrhizobium* sp. (*Lupinus*), 3045USDA wild-type strain (*Rhizobium* Culture Collection, Beltsville, U.S.A.). Lupine nodule primordia are induced just below the zone of emerging root hairs, which was marked at inoculation. The plant growth conditions and bacterial or plant media were as described previously (Łotocka et al., 2000b).

**This work is part of the author's unpublished doctoral dissertation

*e-mail: BŁotocka@gmail.com

SAMPLING OF MATERIAL FOR MICROSCOPY

Three different developmental stages of *Lupinus luteus* L. cv. Ventus nodule were chosen for investigation, and the juvenile stage [by 11 days after inoculation (DAI) as determined by Łotocka et al. (1995)] is reported here. For study of this stage, root fragments ~6 mm below the mark were taken. All samples were fixed and postfixed identically, as described earlier (Łotocka et al., 2000b). Next, the samples were examined under a dissecting microscope and the nodule primordia revealed after osmification were carefully trimmed to suit the intended sectioning planes. The material was gradually dehydrated in ethanol and acetone and embedded in Glycid Ether 100 epoxy resin (SERVA). The samples were positioned in embedding molds to ensure sectioning in transversal, radial or tangential planes versus the root axis. Serial sections 3 µm thick were cut using a Jung-2065-Supercut microtome (Leica/Reichert-Jung) and stained with azure A and methyl blue. For examination of fine structure, ultrathin serial sections were cut with an Ultracut E microtome (Reichert), collected on Formvar-coated slot-grids and contrasted with lead citrate and uranyl acetate.

Observations and microphotographs employed Jenaval (Karl Zeiss Jena) or Axioskop (Zeiss-Opton) light microscopes, or JEM 100C or JEM 1220 (JEOL) transmission electron microscopes (TEM). Negatives were scanned into electronic files (1600 dpi resolution) using a CanoScan 9900F flatbed scanner. The gamma level and contrast of the resulting grey-tone images were adjusted with Adobe Photoshop 7.0 software.

RESULTS

The first root nodule primordia were discernible on taproots by 7 DAI. By 10 DAI, root nodules became slightly pink and were easily discernible at the root surface. By this time, most plants unfolded leaflets of the third leaf.

Formation of the nodule primordium started with centripetal dedifferentiation of the root cortex, discernible 24 h after inoculation in two subrhizodermal cortical layers. The cells were recognized as dedifferentiated when they underwent mitosis or metabolic mobilization was evident, manifested as an increase of cytoplasm volume in comparison to cells in noninfected roots, the formation of numerous small vacuoles and central positioning of the cell nucleus. At 2 DAI, dedifferentiated cells were observed in the 3rd or 4th cortical layer (Fig. 1). In the following days, radially divided derivatives of the 4th and subsequent cortical layers took part in the formation of the nodule vascular system.

Three days after inoculation, bacteroid tissue initials (BTI) encircled by nodule cortex initials (NCI) were already established in subrhizodermal layers, as observed previously (Łotocka et al., 2000b). The cortical derivatives at the proximal side of BTI underwent multiple radial divisions. Simultaneously, numerous cortical cells after a single radial or transversal division were already visible in the layer adjoining the root endodermis, while in the middle cortical layers the divisions were less frequent. In endodermal and pericyclic cells, symptoms of activation were noted, similar to those observed earlier in subrhizodermal cells. In the pericycle, however, initiation of the process was less evidently nodulation-related: as in non-inoculated roots, numerous pericyclic cells, especially at the xylem poles, maintained dense cytoplasm and underwent division sporadically. In inoculated roots, some dense-cytoplasmic or dividing pericycle cells were observed uniformly along the entire nodule initiation zone of the root. Therefore, pericycle dedifferentiation was assumed to be related to the formation of a particular nodule, when at the appropriate xylem pole all the pericycle cells were dedifferentiated. The pericycle was uniseriate except for the xylem poles, where an additional 2–4 layers of parenchymatous cells were present between the endodermis-adjoining pericycle layer and protoxylem. In this work, all these cells are hereafter referred to as multilayered pericycle to simplify the description. Dedifferentiation of the multilayered pericycle was gradual and centripetal. In samples fixed at 3 DAI, only the outer, endodermis-adjoining pericycle layer was dedifferentiated.

In 5-day-old nodule primordia, two zones of frequent cell divisions were discernible. The first one involved the derivatives of the 2nd and 3rd cortical layers (Fig. 2) together with the BTI-flanking derivatives of the 1st layer. The divisions observed in this zone yielded isodiametric cells which did not contribute to vascular tissue formation, as they gave rise subsequently to the nodule cortex. Between zones of frequent divisions, derivative cells of the middle cortical layers divided infrequently and unequally, resulting in the formation of 2–4 files of narrow cells arranged radially between the BTI and the nearest xylem pole (Fig. 2). The second zone of frequent cell divisions adjoined the protoxylem. Here the inner pericycle cells entered dedifferentiation (Fig. 2), and numerous radial divisions occurred in both the outer pericycle layer and endodermis. The tangential divisions of pericycle and endodermis cells characteristic of the development of the lateral root primordium were sporadic in the nodule primordium. Due to mitotic activity in the pericycle and endodermis, fine cambial strands extending radially from the cylindrical root cambium were formed (Fig. 3), to fuse with the above-mentioned files of narrow

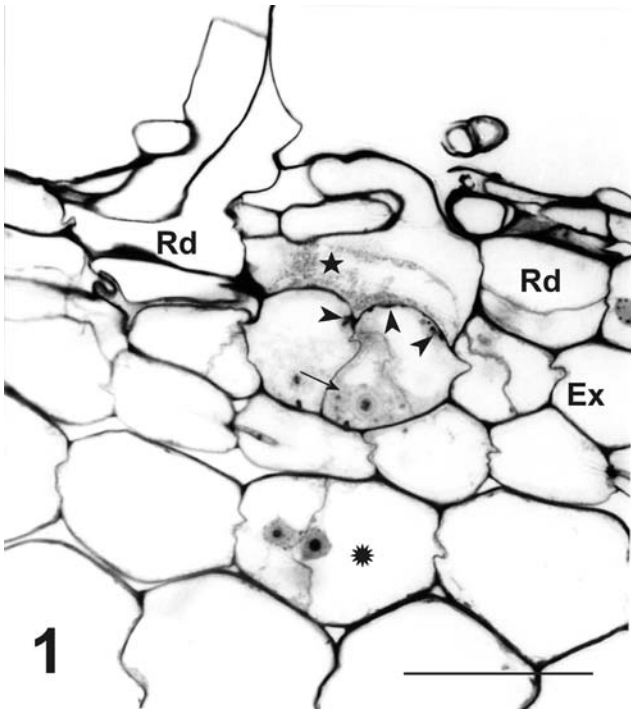
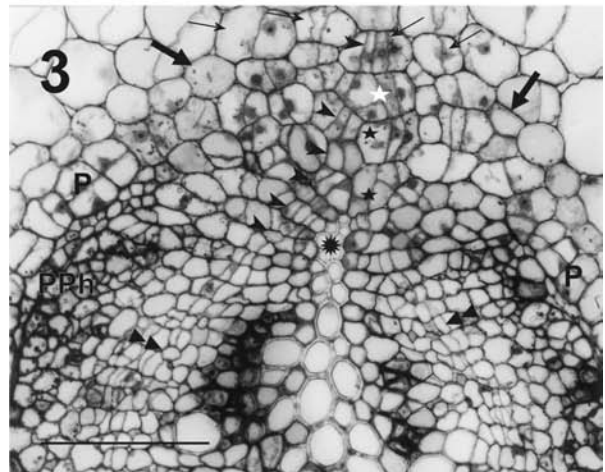
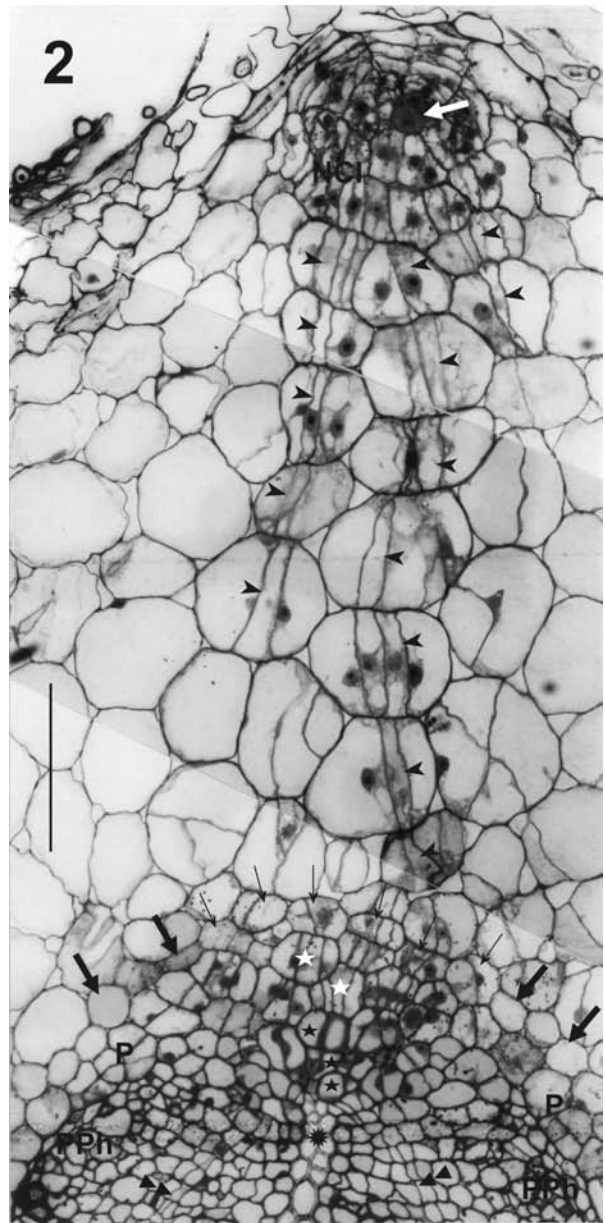


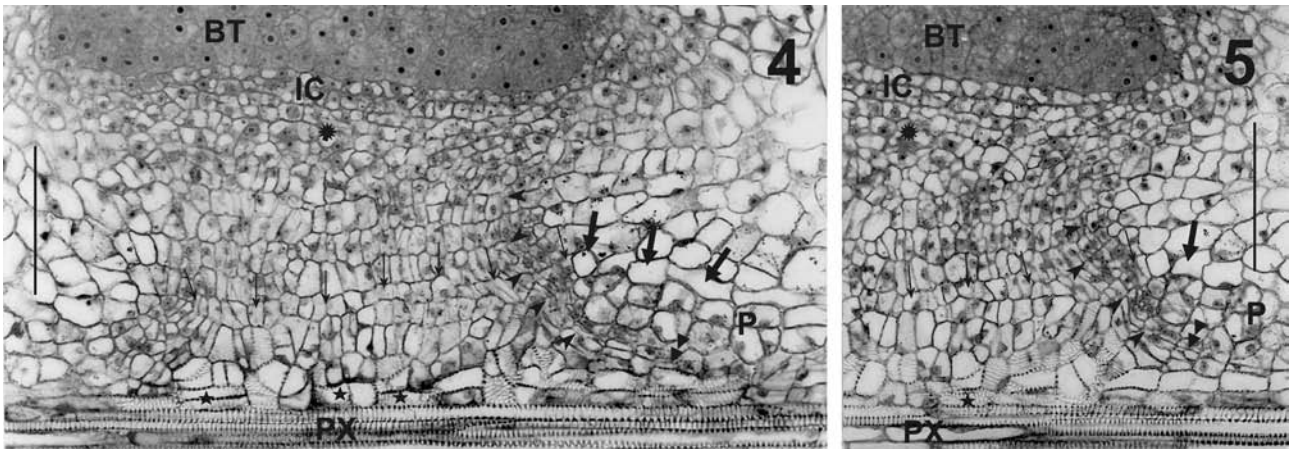
Fig. 1. Root nodule primordium in *Lupinus luteus*, 2 DAI, section transversal to root axis. Ex – exodermis; Rd – rhizodermis; star – increased amount of cytoplasm in basal part of infected root hair cell; arrowhead – local thickenings in cell wall separating infected root hair cell and adjacent cortical cell indicate possible penetration sites; thin arrow – bacteroid tissue initial (BTI); rosette – dedifferentiated cell after single radial division in third layer of root primary cortex. Bar = 65 μ m.

Figs. 2, 3. Root nodule primordium in *Lupinus luteus*, 5 DAI, section transversal to root axis. NCI – nodule cortex initials; P – root pericycle; PPh – primary phloem; white arrow – BTI surrounded with derivatives of 1st, 2nd and 3rd cortical layers after numerous divisions (NCI); arrowheads – files of narrow cells arranged radially between BTI and xylem pole and fused with fine cambial strands extending radially from cylindrical root cambium (double arrowheads); thin arrows – dedifferentiated endodermal cells; arrows – differentiated endodermal cells; white stars – outer pericycle cells after numerous radial divisions; stars – dedifferentiated inner pericycle; rosette – protoxylem tracheary elements. Bars = 130 μ m.

cells. The centripetal wave of cell divisions was reversed at ~5 DAI, as in the next days, within the still-dividing mass of cortical derivatives, a centrifugal wave was evident, proceeding along the files of narrow cells towards the BTI. Therefore it seems reasonable to identify the narrow cells as actual vascular initials of the nodule primordium.

By 7 DAI, the files of vascular initials together with cambial strands extending radially from the





Figs. 4, 5. Root nodule primordium in *Lupinus luteus*, 7 DAI, sections from the same specimen, radial to root axis. BT – bacteroid tissue; IC – inner cortex of nodule; P – root pericycle; PX – primary xylem; arrowheads – cambial strands of NVT arranged radially between young bacteroid tissue and xylem pole and fused with root cambium (double arrowheads); thin arrows – endodermal derivatives after numerous radial divisions; arrows – differentiated endodermal cells; rosette – isodiametric cells in distal part of NVT; stars – short axially arranged (i.e., parallel to protoxylem tracheary elements) tracheids in innermost layer of proximal part of NVT. Note that the derivatives of the other pericycle or endodermal layers are arranged radially. Bars = 120 μ m.

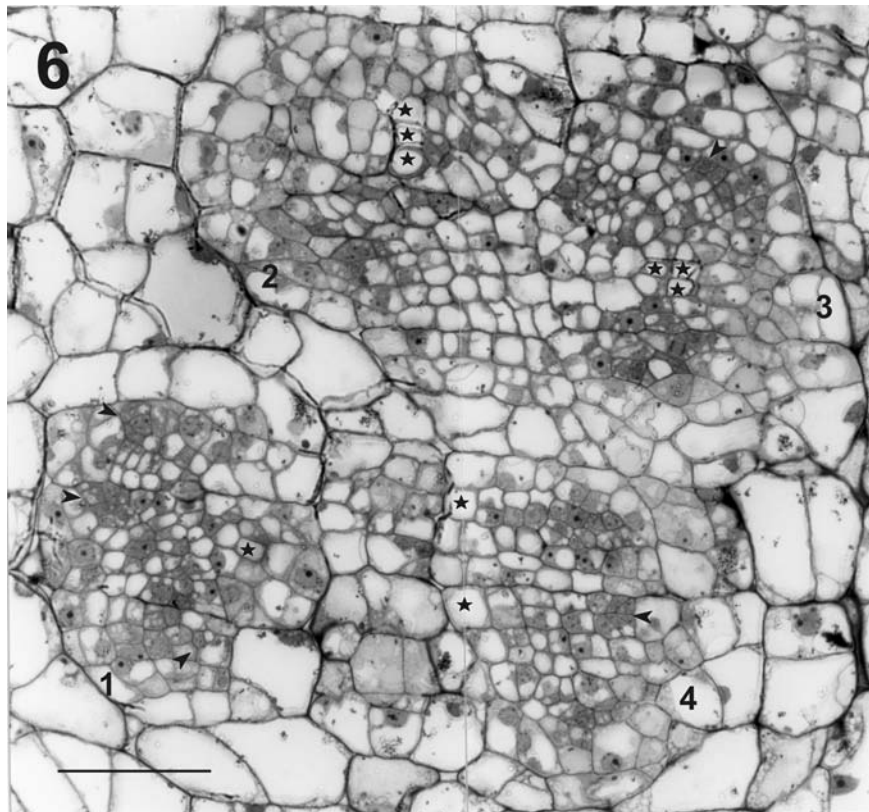


Fig. 6. Middle part of nodule vascular trace in *Lupinus luteus*, 10 DAI, section tangential to root axis. 1–4 – collateral bundles within trace; between differentiating phloem (arrowheads) and xylem already containing tracheary elements visible by LM (asterisks), linearly arranged cambial cells are visible in some places. Note the tendency toward linear arrangement of xylem elements, corresponding to the arrangement of cambial initials. Bar = 65 μ m.

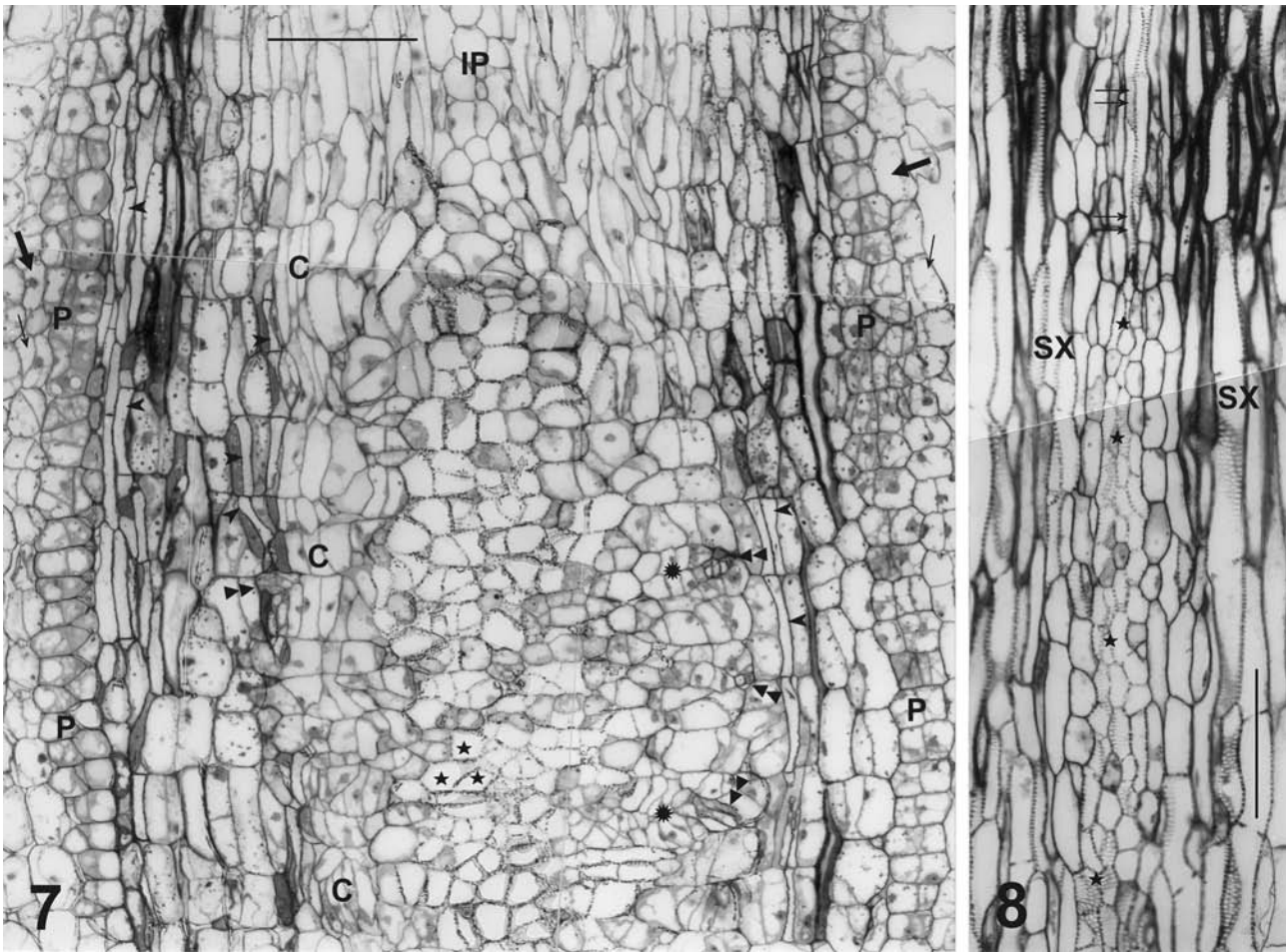
cylindrical root cambium formed the nodule vascular trace (NVT). At this time it was still meristematic and consisted of radially arranged provascular strands, clearly distinct from the other cortical derivatives (Figs. 4, 5). Subsequently, the strands thickened due to longitudinal cell divisions. The derivatives of the 4th cortical layer, which adjoined the initials of nodule inner cortex (the derivatives of the 3rd and 2nd layers), formed the distal part of the NVT. Here the divisions of vascular initials were variously oriented, and all the daughter cells were isodiametric at this time. In the proximal part of the NVT, which was formed from multilayered pericycle derivatives, mature tracheary elements – small and diversely shaped – were discernible by light microscopy. The elements were shorter than those in the root primary or secondary xylem. The innermost ones, which adjoined protoxylem tracheary elements, were parallel to the root axis. The elements that originated from the other pericycle layers (or from endodermal or cortical parenchyma derivatives) were elongated radially according to the NVT orientation. In the tracheary elements originating from the pericycle, the secondary cell wall was irregularly helical or reticulate; it was helical in the elements originating from the endodermis or inner cortex parenchyma.

In the nodule at 10 DAI, as seen in sections tangential to the root axis, the trace usually consisted of four bundles with distinct fascicular cambium (Fig. 6). Also, xylem elements tended toward a linear arrangement, corresponding to the arrangement of cambial initials. Within the vascular trace, xylem elements differentiated centripetally from the cambial zone, and phloem elements differentiated centrifugally; thus the trace's individual bundles were collateral. Tangential sections best showed the organization of the proximal part of the vascular trace. In a trace section cut at the level of root phloem (Fig. 7), numerous small tracheary elements originating from the outer pericycle were visible. In the section shown, there is a disproportion between the number of tracheary (~150) and sieve elements (less than 20); this is characteristic for this part of the nodule trace. The mass of the trace's tracheary elements filled nearly the whole space of the former multilayered pericycle at the protoxylem, in contrast to the sieve elements, which occurred in separate groups, next to the tracheary elements. In cross-section these sieve elements were clearly associated with fine strands of the trace's fascicular cambium branching from the root cambium; this means that the sieve elements were produced by cambial strands, unlike the tracheary elements which differentiated from the mass of multilayered pericycle derivatives. Deeper tangential sections, cut at the root secondary xylem (not shown), showed that at this early stage the inner pericycle-derivative trac-

heary elements were already in contact not only with the protoxylem vessels but also with the newly formed vessels of root secondary xylem. As the former multilayered pericycle narrowed towards the protoxylem, the number of tracheary elements of the trace decreased (Fig. 8), and in the deepest layer their spatial arrangement changed – as observed in radial sections – from radial to axial.

In 10-day-old root nodules, the segmented arrangement of cells, mirroring the arrangement of the original cortical cells, was no longer visible in the NVT. This was the result of frequent multiplanar divisions of the cells differentiating into the trace's vascular parenchyma, and probably also intrusive growth of cambial derivatives of the trace. The process was most evident in the distal part of the vascular trace, where bacteroid tissue was differentiating (Figs. 9, 10). In this part, between 7 and 10 DAI, strands of vascular meristems became evident among the previously identical derivatives of the 4th cortical layer. The strands were formed as extensions of vascular trace bundles, but their direction changed by ~90° versus the (radial) axis of the trace; thus the hitherto parallel trace bundles became separated from one another. These still-meristematic bundles radiated from the trace at the proximal (inner) side of the bacteroid tissue (Fig. 9) towards the nodule meristem (Fig. 11), which at this stage of nodule development took the form of a broad ring encircling the central zone of differentiating bacteroid cells (Fig. 9). The meristematic bundles were separated from bacteroid cells, with frequently dividing inner cortex initials (Fig. 11), and they differed from the surrounding cortex initials in the prevailing division plane. The divisions of cortex initials were anticlinal versus the bacteroid tissue, while longitudinal divisions prevailed in meristematic bundles, consistent with their axis. The meristematic bundles comprised short peripheral cells and elongated central ones (Fig. 11). The short cells subsequently differentiated into the bundles' endodermis and pericycle, and the elongated ones into xylem or phloem. Differentiated tracheary or sieve elements did not occur beyond the site of trace bundle radiation in 10-day-old nodules.

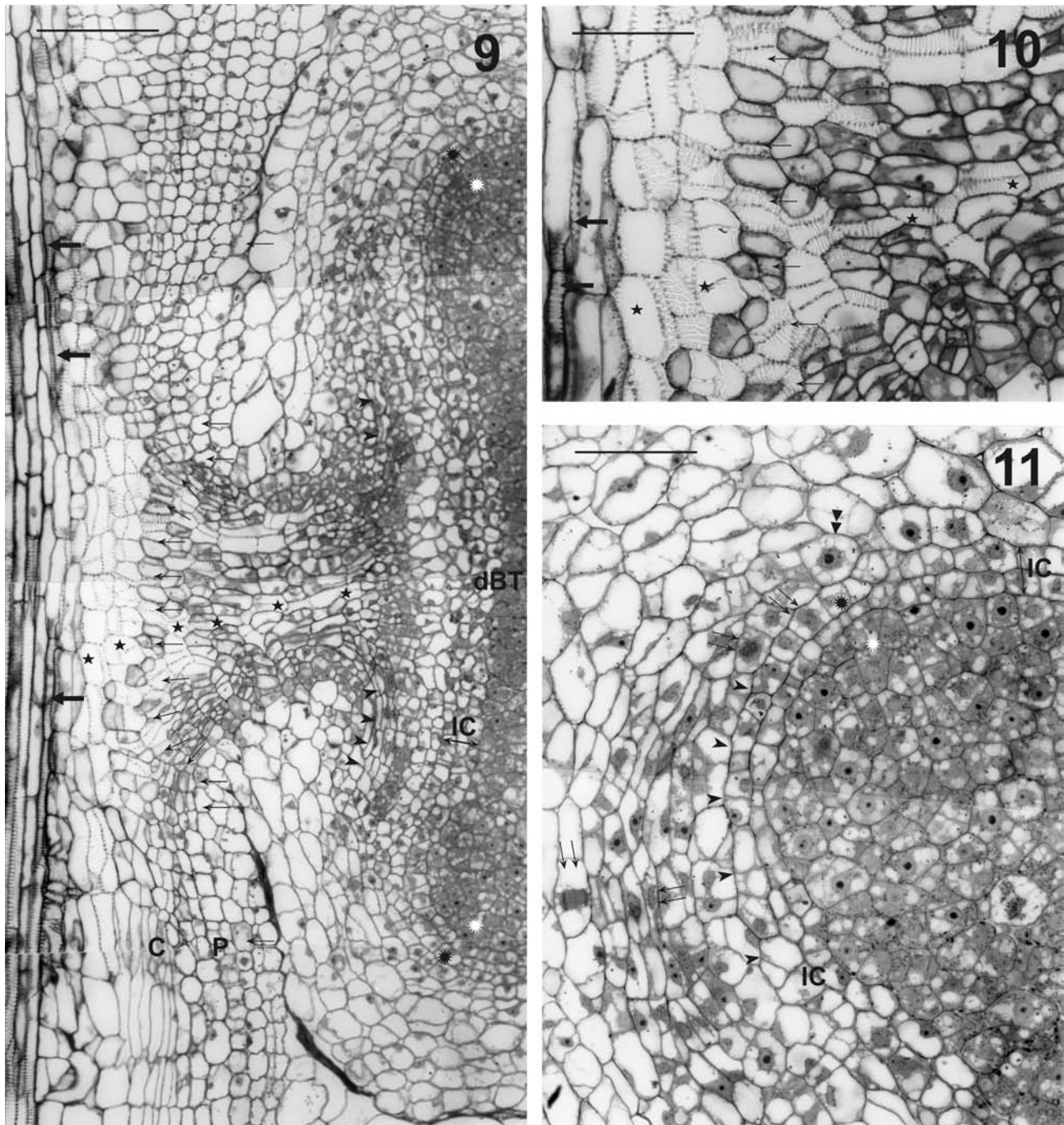
Vascular tissue ultrastructure was examined in detail in 11-day-old nodules. In the proximal part of the NVT, small tracheary elements were accompanied by transfer cells with small wall ingrowths on the wall adjoining the elements (not shown). Differentiating companion cells also formed small wall ingrowths. In the trace's distal part, sieve and tracheary elements differentiated simultaneously within the same bundle. Ultrastructurally, the cells of meristematic bundles were identical to cells of the nodule inner cortex (also meristematic at this stage), except that they lacked large osmiophilic globules at the inner surface of the tonoplast (Fig. 12). At this



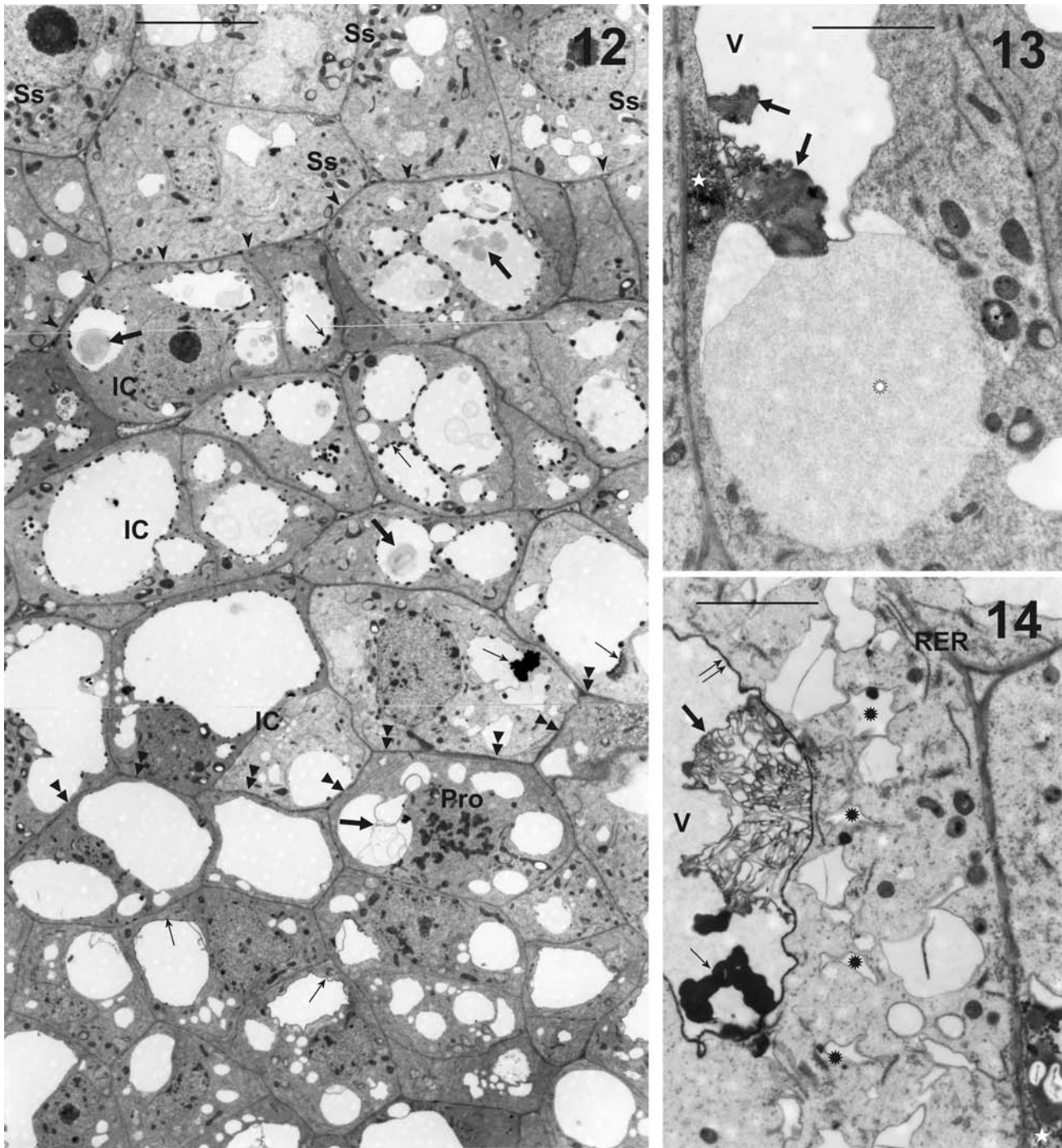
Figs. 7, 8. Nodule vascular trace in its proximal part in *Lupinus luteus*, 10 DAI, section tangential to root axis, cut at the level of root phloem (Fig. 7) or close to root protoxylem (Fig. 8). C – cambium; IP – inner pericycle; P – root pericycle; SX – secondary xylem; arrows – differentiated root endodermis cells; thin arrows – cells of dedifferentiated root endodermis (note dedifferentiation in pericycle also); arrowheads – axially arranged root sieve tubes; stars – numerous small tracheary elements originating from outer pericycle; rosettes – vascular trace cambial strands; double arrowheads – strands of vascular trace's sieve elements; thin double arrows – protoxylem tracheary elements. Note that the arrangement of the trace's tracheary elements changes from radial to axial in the layer adjacent to protoxylem. Bars = 130 μ m.

stage, such osmiophilic globules were as a rule absent from the distal vascular trace or its extensions, but appeared within older, differentiating parts closer to the root stele. Three types of vacuole ultrastructure were recognized in differentiating vascular parenchyma cells. In all cells, a single big vacuole or a few vacuoles of type I were observed (Fig. 13), containing fine, flocculent material and large membranous structures, sometimes myelin-like. Their tonoplast's inner surface usually was covered with a layer of tiny phenolic globules (Fig. 14). Similar globules were often seen in the neighboring cytoplasm (Fig. 13). Vacuoles of type II were less common. They contained fine-granular material resembling autolyzed cytoplasm, and often they adjoined vacuoles of type I (Fig. 13). Vacuoles of type

III, found exclusively in older parenchymatous cells of the trace, were small, irregularly outlined with characteristic narrowings, and contained osmiophilic phenolic deposits in electron-transparent vacuolar sap (Fig. 14). The spatial arrangement of these vacuoles suggested their fusion with vacuoles of type I. The mutual arrangement of type III vacuoles and endoplasmic reticulum (ER) did not support a developmental relationship between them (formation of the vacuoles from ER, for example), as the neighboring ER cisterns were uniformly narrow (Fig. 14) and lacked any osmiophilic content. The diversity of the vacuole of the differentiating vascular parenchyma, the presence of intra-vacuolar myelin-like structures and/or osmiophilic globules were specific exclusively to this stage of nodule vascular system



Figs. 9–11. Vascular system in young root nodules in *Lupinus luteus*, 10 DAI, section radial to root axis. C – cambium; IC – inner cortex of nodule; P – root pericycle; arrows – tracheary elements of root protoxylem; thin arrows – root endodermis and its derivatives, which after numerous radial divisions form a layer within the NVT; stars – trace's differentiated tracheary elements, axially arranged in the innermost part of the trace and radially in the other parts (Fig. 10); arrowheads – strands of vascular meristem within distal part of trace. In Fig. 11, arrowheads are at boundary of vascular meristem strand and inner cortex; white and black rosettes – infected and uninfected cells of nodule meristems, respectively; thin double arrows – dividing cells within vascular or nodule meristem; double arrowhead – terminal cell of vascular meristem strand which could be responsible for its elongation. Bars = 110 μm , 55 μm and 65 μm , respectively.



Figs. 12–14. Ultrastructure of vascular system in young root nodules in *Lupinus luteus*, 11 DAI, section radial to root axis. IC – inner cortex of nodule; Pro – prophase; RER – rough endoplasmic reticulum; Ss – symbiosome; V – vacuole; arrowheads – boundary of bacteroid tissue and inner cortex; double arrowheads – boundary of inner cortex and proximal part of NVT; thin arrows – osmiophilic globules at inner side of tonoplast; arrows – membranous structures within type I vacuoles; white stars – small osmiophilic globules within cytoplasm; white rosette – granular substance within type II vacuole; black rosettes – type III vacuoles. Bars = 10 μm , 3.0 μm and 4.0 μm , respectively.

development; these traits were not observed within the differentiating regions of vascular tissue in older nodules.

In nearly every differentiating parenchymatous cell, small electron-transparent zones appeared within dense chromatin. The zones contained fine-fibrillar material and were separated from the chromatin by invaginations of the inner membrane of the nuclear envelope. Such cell nuclei were found exclusively within nodule vascular tissue, especially at later stages of its development.

DISCUSSION

During meristematic activity related to the initial stages of root nodule vascular system formation in yellow lupine, two stages were distinguished in this work. The first involves localized dedifferentiation of the root primary cortex together with the stelar pericycle, and subsequent differentiation of xylem elements within the dedifferentiated inner pericycle at the root protoxylem. In this location, no new cambial-like organization is observed, and differentiation resembles vascular differentiation in callus (Sachs, 1981). The second stage overlaps the first, and consists in the formation (possibly regulated by a strong polar auxin flux from the root stele) of NVT cambial strands extending from root cambium at the xylem pole towards the BTI, and subsequent formation of the trace's vascular bundles. The first and second stages differ in the direction of the cell division waves – centripetal in the first stage, centrifugal in the second. Also, the new cells appearing during the first stage are direct derivatives of the original root tissues, while in the second stage the new cells are produced by a specialized vascular meristem: fascicular cambium of the NVT.

Simple handbook definitions and terminology cannot be unambiguously applied to initiation of the vascular meristem in the root nodule primordium of lupine. Under non-stress conditions, vascular tissues are produced by two meristems, either the primary procambium or secondary cambium (Esau, 1953). The terms "primary" and "secondary" indicate the relative time of appearance of these meristems in a specific plant organ. The additional parts of the plant body that may be formed after the primary structures have appeared are termed "secondary," as are the meristems that give rise to them. Thus, the secondary meristems correspond to typically lateral meristems: vascular cambium and phellogen. In older handbooks, secondary meristems were distinguished depending on their genesis through dedifferentiation of mature tissues. As shown in this work on lupine, the meristem that produces the nodule vascular system arises due to the dedifferentiation of at least two mature tissues of root – corti-

cal parenchyma and endodermis (the root pericycle that is also involved in the process may be considered part of the temporarily inactive root procambium) – after the primary structure of the root is established. Thus the meristem is undoubtedly of secondary origin. Should it be classified as vascular cambium? Such a classification seems inappropriate, as the organization of initials within the nodule vascular meristem differs from lupine root or stem cambium. The indeterminately functioning root or stem cambium is cylindrical, and the fusiform initials and ray initials produce a voluminous mass of secondary vascular tissues with a specific three-dimensional arrangement of conductive, parenchymatous and mechanical elements. In contrast, the root nodule vascular meristem produces thin strands of vascular tissues in the form of collateral bundles which completely lack the mechanical elements in yellow lupine. Nodule vascular meristem differentiates early in its peripheral part into pericyclic parenchyma cells (root or stem cambium does not produce such a tissue), and its mitotic activity, if maintained, occurs only in the bundles' central part, leading to a linear arrangement of xylem cells. Thus, the nodule vascular meristem rather resembles fascicular cambium.

Another complication in classifying the nodule vascular meristem is related to the genesis of nodule bundles, which differs from that of the NVT. As already visible in nodules at 10 DAI (and especially in older nodules; see Part 2), after being initiated within the distal part of the NVT they are elongated through the activity of nodule meristems. In lupine these meristems are two-layered, with an outer non-infected cell layer giving rise to the nodule inner cortex; discrete vascular initials presumably are present in this outer layer. The process of nodule bundle elongation resembles the formation of procambial strands within stem apical buds, in that vascular meristem elongation proceeds toward the meristem (Esau, 1953; Hejnowicz, 1980). In the case of nodule bundles, it is reasonable to presume a determinative polar auxin flux (which controls primary stem vascularization) occurring from the stem via root stele, NVT and nodule bundles towards the nodule meristems.

In light of the above, the term "fascicular cambium" used in this work seems more appropriate than "vascular cambium" to designate the meristematic cells that produce the different parts of the nodule vascular system.

To what extent does the formation of the lupine nodule vascular system described in this study resemble the same process in the root nodules of other legumes? There are no data on vascular differentiation in determinate-type nodules initiated in the outer cortex, as in lupines. The root nodule vascular system of clover is relatively well studied. The

root nodules of clover and lupine are of indeterminate type (Łotocka et al., 1997; Golinowski et al., 1987). In clover, however, the cylindrical root nodule is initiated in the inner cortex, unlike lupinoid nodules. The role of the root endodermis is different in clover root nodule morphogenesis. In lupine, as shown in this work, cell divisions are equally frequent in the endodermis and in the cortical parenchyma or pericycle, and consequently the endodermal derivatives take part in formation of the NVT. In clover the endodermis dedifferentiates but its mitotic activity ceases and the layer of endodermal derivatives becomes discontinuous as it becomes separated by the pericycle derivatives that form the vascular connection between the root vascular system and the nodule (Łotocka et al., 1997).

ACKNOWLEDGEMENTS

I thank Dr. Ewa Kurczyńska for helpful comments on the manuscript, and Ewa Znojek and Alicja Żuchowska for expert technical assistance.

REFERENCES

- BRENCHLEY WW, and THORNTON HG. 1925. The relation between the development, structure and functioning of the nodules of *Vicia faba* as influenced by the presence or absence of boron in the nutrient medium. *Proceedings of the Royal Society of London. Series B, Biological Sciences* 98: 373–398.
- BRIARTY LG. 1978. The development of root nodule xylem transfer cells in *Trifolium repens*. *Journal of Experimental Botany* 29: 735–747.
- ESAU K. 1953. *Plant anatomy*. John Wiley & Sons, Inc., Chapman & Hall, Ltd., New York, London.
- FRASER HL. 1942. The occurrence of endodermis on leguminous root nodules and its effect upon nodule function. *Proceedings of the Royal Society of Edinburgh, B*. 61: 328–343.
- FRED EB, BALDWIN IL, and MCCOY E. 1932. Root nodule bacteria and leguminous plants. *University of Wisconsin Studies in Science* 5: 1–343.
- GOLINOWSKI W, KOPCIŃSKA J, and BORUCKI W. 1987. The morphogenesis of lupine root nodules during infection by *Rhizobium lupini*. *Acta Societatis Botanicorum Poloniae* 56: 687–703.
- GOLINOWSKI W, KOPCIŃSKA J, and BORUCKI W. 1992. Morphometric characteristics of bacteroidal tissue in yellow lupine (*Lupinus luteus* L.) nodules. *Acta Societatis Botanicorum Poloniae* 61: 307–318.
- HEJNOWICZ Z. 1980. *Anatomia i histogeneza roślin naczyniowych*. Państwowe Wydawnictwo Naukowe, Warszawa.
- HIRSCH AM. 1992. Developmental biology of legume nodulation. *New Phytologist* 122: 211–237.
- ŁOTOCKA B, ARCISZEWSKA-KOZUBOWSKA B, DĄBROWSKA K, and GOLINOWSKI W. 1995. Growth analysis of root nodules in yellow lupin. *Annals of Warsaw Agricultural University – SGGW, Agriculture* 29: 3–12.
- ŁOTOCKA B, KOPCIŃSKA J, BORUCKI W, STĘPKOWSKI T, ŚWIDERSKA A, GOLINOWSKI W, and LEGOCKI AB. 2000a. The effects of mutations in *nolL* and *nodZ* genes of *Bradyrhizobium* sp. WM9 (*Lupinus*) upon root nodule ultrastructure in *Lupinus luteus* L. *Acta Biologica Cracoviensia Series Botanica* 42: 155–163.
- ŁOTOCKA B, KOPCIŃSKA J, and GOLINOWSKI W. 1997. Morphogenesis of root nodules in white clover. I. Effective root nodules induced by the wild type of *Rhizobium leguminosarum* biovar. *trifolii*. *Acta Societatis Botanicorum Poloniae* 66: 273–292.
- ŁOTOCKA B, KOPCIŃSKA J, GÓRECKA M, and GOLINOWSKI W. 2000b. Formation and abortion of root nodule primordia in *Lupinus luteus* L. *Acta Biologica Cracoviensia Series Botanica* 42: 87–102.
- PATE JS, GUNNING BES, and BRIARTY LG. 1969. Ultrastructure and functioning of the transport system of the leguminous root nodule. *Planta* 85: 11–34.
- SACHS T. 1981. The control of the patterned differentiation of vascular tissues. *Advances in Botanical Research* 9: 151–262.